TRENDS IN SCIENCES 2026; 23(2): 11128
https://doi.org/10.48048/tis.2026.11128 RESEARCH ARTICLE

# Bacterial Cellulose Production in Thai Red Tea Fermentation: Role of Sucrose-Based Sugar Combinations as Carbon Sources

**Wawan Agustina[1,2] and Apichat Boontawan[1,*]**

[1]*School of Biotechnology, Institute of Agricultural Technology, Suranaree University of Technology, Nakhon Ratchasima 30000, Thailand*
[2]*Research Center for Food Technology and Processing, National Research and Innovation Agency (BRIN), Daerah Istimewa Yogyakarta 55861, Indonesia*

**([*]Corresponding author's e-mail: apichat@sut.ac.th)**

*Received: 30 June 2025, Revised: 5 August 2025, Accepted: 15 August 2025, Published: 1 November 2025*

**Abstract**

Bacterial cellulose (BC) is a versatile biopolymer produced via microbial fermentation, valued for its purity, strength, and biocompatibility. In this study, BC was synthesized using Thai red tea as the fermentation medium, combined with various carbon source combinations: Control (RTC-C), sucrose-dextrose (RTC-SD), sucrose-glucose (RTC-SGlu), sucrose-fructose (RTC-SF), and sucrose-glycerol (RTC-SGly). Fermentation was carried out for 15 days at ~30 °C using a tea solution (1% w/v), total sugar content of 10% (w/v), and 10% (v/v) kombucha culture. The resulting BC was evaluated for yield, morphology, structure, and thermal/mechanical properties using SEM, FTIR, XRD, and TGA analysis. Carbon source combinations significantly influenced BC production, with wet and dry yields ranging from 74.53 g/L and 0.66 g/L (RTC-SGly) to 259.54 g/L and 2.59 g/L (RTC-SGlu), respectively. The sucrose-glucose combination yielded the highest productivity. SEM revealed a uniform nanofiber network with fiber diameters ranging from 29.70 ± 5.17 nm to 40.39 ± 8.65 nm. FTIR and XRD confirmed the formation of cellulose type I, with crystallinity indexes ranging from 84.74% (RTC-SGly) to 88.35% (RTC-SF). Thermal and mechanical properties were comparable across all samples. These findings demonstrate that specific carbon source combinations, particularly sucrose-glucose and sucrose-dextrose, can significantly enhance BC yield without compromising its structural integrity, highlighting their potential for industrial-scale applications.

**Keywords:** Bacterial cellulose, Kombucha fermentation, Carbon source combinations, Thai red tea, Cellulose production, Structural, Mechanical properties

## Introduction

Bacterial cellulose (BC) is a nanostructured exopolysaccharide synthesized by specific acetic acid bacteria, particularly those from the *Komagataeibacter* genus. Compared to plant-derived cellulose, BC exhibits superior characteristics, including high crystallinity, tensile strength, purity, water-holding capacity, and biocompatibility. These features make it a valuable biomaterial across various industries, including food, biomedical, packaging, and cosmetic [1-4].

Kombucha fermentation has recently gained interest as an alternative biotechnological platform for BC production. This fermentation process involves a symbiotic culture of bacteria and yeast (SCOBY) cultivated in a tea-based medium under static aerobic conditions. The yeasts hydrolyze sucrose into glucose and fructose, which are then utilized by acetic acid bacteria for cellulose biosynthesis. The microbial synergy within the SCOBY plays a critical role in cellulose production, particularly when supported by suitable carbon sources and nutrient-rich tea infusions [5-7].

Among available substrates, tea infusions derived from *Camellia sinensis*—such as green, black, and oolong teas—have been widely used due to their content

of polyphenols, amino acids, and minerals that promote microbial growth and activity [8]. In our previous work, Thai red tea (*Camellia sinensis*) was identified as a highly effective and economical fermentation medium for BC production, offering both strong microbial support and cost advantages over other tea types.

While the fermentation matrix contributes essential nutrients, the type and composition of the carbon source remain primary determinants of BC yield and quality. Sugars not only serve as energy sources but also act as direct precursors in the cellulose biosynthetic pathway via the UDP-glucose route [9,10]. Although many studies have investigated the impact of individual sugars—such as glucose, fructose, dextrose, glycerol, or sucrose—on BC production, the use of sugar combinations remain relatively unexplored, particularly in kombucha systems. Considering that sucrose is naturally hydrolyzed during kombucha fermentation, combining it with other sugars may influence microbial interactions, carbon utilization, and ultimately, cellulose biosynthesis [11-13].

Building on this perspective, the present study investigates the effects of various sucrose-based sugar combinations—specifically with glucose, fructose, dextrose, and glycerol—on the production and characteristics of BC in Thai red tea kombucha fermentation. By systematically evaluating these combinations, this work aims to provide new insights into optimizing carbon source formulations for enhanced BC yield and quality. The findings are expected to support future optimization studies and contribute to the development of low-cost, scalable BC production systems using tea-based fermentation platforms.

## Materials and methods

The materials used in this study included a commercial kombucha starter (SCOBY) from Neo Cold Brew Shop (Thailand), Thai red tea-vanilla flavor (*ChaTraMue* brand), and commercial white sugar (sucrose). Additional chemicals were NaOH (Q RëC™), D-glucose (UniVAR, Merck), D-fructose (Carlo Erba), sucrose (ACI Labscan), dextrose monohydrate (KC, Bangkok Chemical), and glycerol (Merck). Reverse osmosis (RO) and deionized (DI) water were used as water sources. The equipment included a cheesecloth, coffee filter, glass jar, funnel, autoclave (Biobase), laboratory glassware, biosafety cabinet (Cryste, Puricube Neo), analytical balance (AE Nimbus NBL 84E), incubator, pH meter (Oakton pH 700), refractometer, oven dryer (XUE058, France-Etuves), FT-IR (Bruker VERTEX 70), XRD (Bruker D8 Advance), SEM (Zeiss AURIGA, Germany), nanoindenter (NanoTest Vantage, Micro Materials Limited, UK), and HPLC (Hitachi Chromaster).

### Bacterial cellulose production

The fermentation medium was prepared by dissolving 20 g of sucrose in 180 mL of Thai red tea extract (10 g/L), which was obtained by steeping 2 g of tea in 180 mL of hot deionized water (90 °C, 15 min), followed by filtration and mixing with sucrose. The volume was adjusted to 180 mL, stirred, autoclaved (121 °C, 15 min), and cooled to 30 - 35 °C.

For starter regeneration, 20 mL of commercial kombucha was added to the prepared medium and incubated statically at 30 °C for 14 days. For BC production, 20 mL of the regenerated starter was inoculated into fresh media containing different carbon sources and incubated statically at 30 °C for 15 days.

To investigate the effect of carbon source combinations on BC production, five types of fermentation media were used. The control treatment (RTC-C) contained 10 g/100 mL sucrose. The other treatments consisted of a 1:1 mixture of sucrose (5 g/100 mL) with either fructose (RTC-SF), dextrose (RTC-SD), glycerol (RTC-SGly), or glucose (RTC-SGlu), keeping the total carbon source concentration at 10 g/100 mL in all cases.

Following fermentation, BC pellicles were harvested, boiled for 30 min, treated with 2% NaOH at 90 °C for 120 min, rinsed with deionized water to neutral pH, drained, weighed (wet weight), and oven-dried at 40 °C to constant weight using a method modified from [14]. All treatments were performed in triplicate to ensure reproducibility.

### Culture medium characterization

Before and after fermentation, the culture medium was analyzed for Brix, pH, and sugar content, including sucrose, glucose, fructose, and glycerol. Brix was measured using a refractometer, and pH was determined using a pH meter. Sugar analysis was performed using an HPLC system equipped with an Aminex HPX-42A

column and a refractive index detector (RI). Filtered deionized water (0.22 µm) served as the mobile phase, operated at a flow rate of 0.6 mL/min for 22 min with the column maintained at 45 °C. Samples were diluted (1:10), filtered through a 0.22 µm membrane, and quantified against a standard curve (0 - 15 g/L). All measurements were carried out in triplicate to ensure reproducibility and accuracy after system stabilization.

**Bacterial cellulose characterization**

***Visual appearance of BC***

The visual appearance of BC samples was assessed before and after purification with NaOH to evaluate any changes in color. All observations were conducted under uniform lighting conditions through direct visual inspection. Each sample was compared to the control (RTC-C) to identify noticeable differences in coloration.

***Yield and water holding capacity analysis***

Following purification, the BC samples were drained for approximately 10 min before being weighed to determine the wet weight (wet yield). For dry weight (dry yield) measurement, the samples were oven-dried at 40 °C until a constant weight was reached, following the method described by Aswini *et al.* [14]. The water holding capacity (WHC) was calculated based on the amount of water lost during drying and expressed as the ratio of water weight to dry BC weight (g/g), as described by Schrecker and Gostomski [15]. All measurements were performed in triplicate.

***Morphology and fiber size analysis***

The surface morphology of BC was analyzed via scanning electron microscopy (SEM). Dried BC sheets were cut into ~5×5 mm pieces, mounted on SEM stubs, and gold-coated. Fiber diameters were measured from SEM images using ImageJ software, based on 50 data points per sample [16]. Statistical analysis was performed using one-way ANOVA followed by an LSD test ($p < 0.05$) to compare differences between groups.

***FT-IR spectroscopy analysis***

The functional groups present in the samples were analyzed using Fourier-transform infrared (FT-IR) spectroscopy. Spectra were collected in transmittance mode across the range of 400 to 4,000 $cm^{-1}$, with a resolution of 4 $cm^{-1}$. Each spectrum was obtained by averaging 64 scans for both the background and the sample. All measurements were conducted at ambient (room) temperature.

***X-Ray diffraction analysis***

X-ray diffraction (XRD) analysis was performed using a Bruker D8 Advance diffractometer to investigate the crystalline characteristics of the samples, including diffraction peaks (2θ) and crystallinity index (CI). The instrument operated at 40 kV and 40 mA (1,600 W), scanning across a 2θ range of 10° to 60°. Data were collected in 2,446 steps, with each step sized at 0.0204° and a scan duration of 0.4 s, totaling approximately 1,035.2 seconds per sample. The CI was determined using Equation 1, while crystallite size was calculated via the Scherrer equation Eq. (2). Further analysis of crystallinity and crystallite dimensions was carried out using *OriginLab* and *Microsoft Excel.*

$$CI = \frac{Total\ Area\ of\ Crystalline\ Peak}{Total\ Area\ of\ Crystalline\ and\ Amorphous\ Peaks} \times 100\% \quad (1)$$

$$d = \frac{K\lambda}{\beta\ cos\ \theta} \quad (2)$$

where CI is the crystallinity index, d is the crystallite size, K is the Scherrer constant (0.89), λ is the X-ray wavelength (1.5406 Å), β is the full width at half maximum (FWHM) in radians, and θ is the Bragg angle [17].

***Thermogravimetric analysis***

A thermogravimetric analyzer (Mettler-Toledo, Model TGA/DSC1) was used to assess the dynamic weight loss and thermal degradation behavior of BC samples. The samples were heated in an alumina pan at a temperature of 10 °C per min from 28 °C to 600 °C while flowing at a rate of 30 mL/min in a nitrogen ($N_2$) environment. *OriginLab* software was used to process TGA/DTG data, and *Microsoft Excel* was used to create the associated graphs.

***Nano-indentation***

The mechanical characteristics of BC films were examined using a nanoindenter. Circular samples approximately 0.8 cm in diameter were prepared and securely attached to the holder with white adhesive

latex. Indentation testing involved applying a maximum load of 50 mN with a loading and unloading speed of 0.40 mN/s. To ensure reliability, 6 indentations were conducted on each sample, and the average values were recorded. Young's modulus ($E$) was determined using the following formula Eq. (3):

$$E = \frac{(1-v^2)}{\left(\frac{1}{E_r} - \frac{(1-v_i^2)}{E_i}\right)} \quad (3)$$

where $v$ represents the Poisson's ratio of the BC sample (0.3), $E_r$ is the reduced modulus, $v_i$ denotes the Poisson's ratio of the indenter (0.07), and $E_i$ is the Young's modulus of the indenter (1141 GPa) [18,19].

***Statistical analysis***

All experiments were conducted with an appropriate number of replications depending on the parameter measured. Most measurements were performed in triplicate, fiber diameter analysis involved 50 measurements per sample, and nanoindentation tests were conducted with 6 replications. Data are expressed as mean ± standard deviation (SD). Statistical analyses were performed using Microsoft Excel. One-way analysis of variance (ANOVA) was used to assess differences among treatments, followed by the Least Significant Difference (LSD) test for post-hoc comparisons. Statistical significance was determined at a 95% confidence level ($p < 0.05$).

**Results and discussion**

**Characteristics of culture medium**

***The change of pH and total soluble solid (TSS)***

This study investigated pH and TSS changes during fermentation (**Table 1**). The initial medium pH (4.57 - 4.84) dropped slightly to 3.61 - 3.66 after inoculation, then declined significantly to 2.17 - 2.66 over 15 days. Among carbon sources, RTC-SGLU yielded the lowest final pH, while RTC-SGly had the highest. The initial pH drop is attributed to the starter culture's acidic nature, with further reduction driven by organic acid production (e.g., acetic, gluconic, lactic, and citric acids) [14,20]. Similar trends were reported in kombucha fermentation, with pH decreasing from 3.04 to 2.63 after 10 days [21]. Other studies noted final pH ranges of 3.36 - 3.82 [22] and 2.72 - 2.79 [23], consistent with typical acidification during fermentation.

This study monitored changes in pH and total soluble solids (TSS) during fermentation (**Table 1**). The initial pH of the medium (ranging from 4.57 to 4.84) decreased slightly to 3.61 - 3.66 after inoculation, then dropped significantly to 2.17 - 2.66 by day 15. Among the carbon source treatments, RTC-SGlu resulted in the lowest final pH, while RTC-SGly had the highest. The initial pH reduction is likely due to the acidity of the starter culture, while the continued decline is attributed to the production of organic acids such as acetic, gluconic, lactic, and citric acids [14,20]. Similar acidification patterns have been reported in previous kombucha studies, with pH decreasing from 3.04 to 2.63 after 10 days [21], and final pH values ranging from 3.36 to 3.82 [22] and 2.72 to 2.79 [23], aligning with the typical pH decline observed during fermentation.

**Table 1** Changes in pH and Brix degree during kombucha RTC fermentation with different additives.

| Samples | The Change of the pH | | | The Change of the Brix | | |
|---|---|---|---|---|---|---|
| | Medium | Before | after | Medium | Before | after |
| RTC-C | 4.84 ± 0.00$^{d}$ | 3.65 ± 0.00$^{c}$ | 2.52 ± 0.04$^{c}$ | 10.70 ± 0.00$^{d}$ | 10.60 ± 0.00$^{c}$ | 8.57 ± 0.05$^{c}$ |
| RTC-SD | 4.76 ± 0.00$^{b}$ | 3.62 ± 0.00$^{b}$ | 2.21 ± 0.0$^{a}$ | 10.10 ± 0.00$^{b}$ | 10.10 ± 0.00$^{b}$ | 8.33 ± 0.09$^{a}$ |
| RTC-SF | 4.57 ± 0.00$^{a}$ | 3.61 ± 0.00$^{a}$ | 2.46 ± 0.01$^{b}$ | 10.50 ± 0.00$^{c}$ | 10.40 ± 0.00$^{a}$ | 7.87 ± 0.12$^{b}$ |
| RTC-SGlu | 4.76 ± 0.00$^{b}$ | 3.62 ± 0.00$^{a}$ | 2.17 ± 0.01$^{a}$ | 10.70 ± 0.00$^{d}$ | 10.40 ± 0.00$^{b}$ | 8.40 ± 0.08$^{a}$ |
| RTC-SGly | 4.78 ± 0.00$^{c}$ | 3.66 ± 0.00$^{c}$ | 2.66 ± 0.00$^{d}$ | 9.70 ± 0.00$^{a}$ | 9.70 ± 0.00$^{c}$ | 8.60 ± 0.00$^{d}$ |

Different lowercase superscript letters within the same column indicate significant differences among the tea samples (LSD test, $p < 0.05$).

For the TSS observation, initial values ranged from 9.70 ± 0.00 to 10.70 ± 0.00° Brix before inoculation. After adding the inoculum, the TSS remained relatively stable, ranging from 9.70 ± 0.00 to 10.60 ± 0.00° Brix. However, by the end of the fermentation process, TSS values decreased significantly, reaching a range of 8.57 ± 0.05 to 8.60 ± 0.00° Brix.

This reduction reflects microbial sugar consumption, where microorganisms metabolize sugars for growth, energy, and the production of metabolites such as organic acids, ethanol, and BC [13]. Carbon sources like glucose, fructose, and glycerol are converted into intermediates that fuel BC biosynthesis, a process driven by microbial activity [24]. Similar trends have been reported in other fermentations, such as snake fruit kombucha (TSS decline from 13.30 - 14.08 to 12.43° - 12.97° Brix [25]) and cascara kombucha (10.97° to 9.97° Brix over 6 days [24]). These findings highlight the consistent role of microbial activity in reducing sugar content during fermentation [26].

***The change of sugar composition***

HPLC analysis revealed significant changes in sugar profiles (**Table 2**). Initial concentrations ranged from 4.41% -9.05% sucrose, 0.82% - 5.16% glucose, 0% - 4.92% fructose, and 5.40% glycerol (RTC-SGly). Glucose and fructose in samples without added glucose/dextrose resulted from sucrose hydrolysis during autoclaving and kombucha culture activity. Previous studies confirm similar findings, with autoclaving a 3% sucrose solution yielding 0.7% - 0.9% glucose [27] and full sucrose hydrolysis at pH 2 [28].

Sucrose serves as the primary carbon source, enzymatically hydrolyzed to glucose and fructose by yeast invertase [29,30]. Microorganisms exhibit preferential uptake of monosaccharides, with glucose being rapidly metabolized through glycolysis [29]. Under anaerobic conditions, yeasts ferment hexoses to ethanol, which acetic acid bacteria subsequently oxidize to acetic acid [31]. This metabolic hierarchy explains the differential sugar utilization rates: Glucose (57.0% ± 0.5%) and dextrose (51.9% ± 0.3%) were most rapidly consumed, followed by fructose (41.1% ± 0.4%), while sucrose (22.1% ± 0.2%) and glycerol (19.6% ± 0.1%) showed significantly lower reductions ($p < 0.05$, ANOVA). These results align with Neffe-Skocińska *et al.* [21], who reported 92.6% sucrose depletion (9.97% - 0.74%), minimal glucose change (0.09% - 0.10%), and 12.4-fold fructose accumulation (0.07% - 0.87%) in kombucha fermentation.

**Table 2** The change of sugar composition during Thai red tea kombucha fermentation with different types of carbon sources.

| Samples | Before fermentation | | | | After fermentation | | | |
|---|---|---|---|---|---|---|---|---|
| | Sucrose | Glucose | Fructose | Glycerol | Sucrose | Glucose | Fructose | Glycerol |
| RTC-C | $9.05 \pm 0.18^{b,B}$ | $2.13 \pm 0.02^{b,B}$ | $1.05 \pm 0.03^{c,A}$ | ND | $7.05 \pm 0.21^{d,A}$ | $1.89 \pm 0.08^{b,A}$ | $0.74 \pm 0.20^{b,A}$ | ND |
| RTC-SF | $4.68 \pm 0.29^{a,B}$ | $0.82 \pm 0.23^{a,A}$ | $4.92 \pm 0.28^{d,B}$ | ND | $3.53 \pm 0.06^{b,A}$ | $1.02 \pm 0.03^{a,A}$ | $2.89 \pm 0.28^{c,A}$ | ND |
| RTC-SD | $4.75 \pm 0.26^{a,B}$ | $4.91 \pm 0.20^{c,B}$ | $0.37 \pm 0.20^{b,A}$ | ND | $2.30 \pm 0.29^{a,A}$ | $2.36 \pm 0.27^{bc,A}$ | $0.83 \pm 0.13^{b,B}$ | ND |
| RTC-SG | $4.72 \pm 0.51^{a,B}$ | $5.16 \pm 0.54^{c,B}$ | $0.33 \pm 0.16^{b,A}$ | ND | $2.00 \pm 0.20^{a,A}$ | $2.22 \pm 0.10^{b,A}$ | $0.92 \pm 0.16^{b,B}$ | ND |
| RTC-SGly | $4.41 \pm 0.07^{a,A}$ | $1.06 \pm 0.03^{a,A}$ | $0.00 \pm 0.00^{a,A}$ | $5.40 \pm 0.23^{B}$ | $3.89 \pm 0.29^{c,A}$ | $0.92 \pm 0.08^{a,A}$ | $0.00 \pm 0.00^{a,A}$ | $4.34 \pm 0.18^{A}$ |

Different lowercase letters in columns indicate significant differences among tea samples ($p < 0.05$), while uppercase letters in rows indicate significant differences between pre- and post-fermentation ($p < 0.05$, LSD test). ND = not detected.

**Characteristics of bacterial cellulose**

***The appearance of bacterial cellulose***

The appearance of BC produced from Thai red tea kombucha fermentation with different uses of carbon source combinations is presented in **Figure 1.** Unpurified BC from RTC-SD, RTC-SGlu, and RTC-SF appears darker red-orange compared to RTC-C and RTC-SGly (**Figures 1(a) and 1(b)**). This color likely results from natural tea pigments and artificial colorants in Thai red tea, which contains black tea, artificial flavor, and FD&C Yellow No. 6 (INS 110). Black tea catechins oxidize into theaflavins (reddish-orange) and thearubigins (brown) [32,33], while FD&C Yellow No. 6 enhances the orange-red hue [32-34]. After purification with 2% w/v sodium hydroxide, the BC turns white (**Figure 1(c)**) and retains a consistent white, opaque color after oven drying at 40 °C (**Figure 1(d)**), matching findings in most BC studies. Sodium hydroxide effectively removes tannins, polyphenols, residual bacteria, yeast cells, proteins, nucleic acids, and other organic compounds from the kombucha pellicle [35,36].

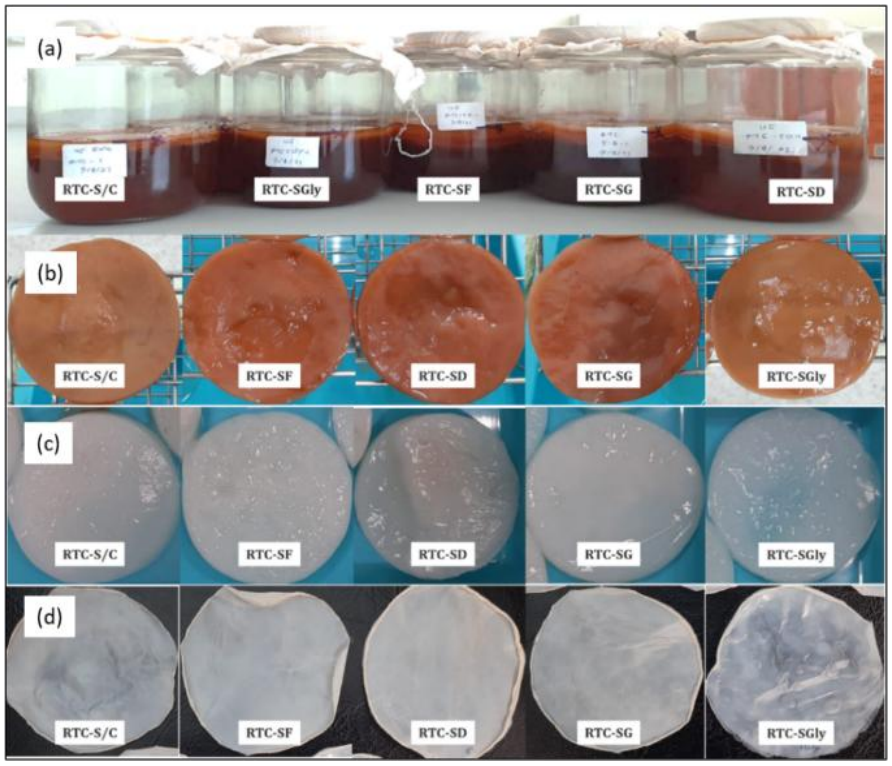


**Figure 1** BC appearance at different stages of Thai red tea kombucha fermentation with various carbon source combinations: (a) during fermentation, (b) before purification, (c) after purification with sodium hydroxide, and (d) after oven drying.

***BC productivity and water holding capacity***

**Figure 2** demonstrates the wet yield, dry yield, and WHC of BC in Thai red tea fermentation with different carbon source combinations. Among the treatments, RTC-SGlu showed the highest wet and dry BC yields, significantly exceeding RTC-C, RTC-SF, and RTC-SGly ($p < 0.05$), but not differing from RTC-SD ($p > 0.05$). This result likely reflects the efficient microbial metabolism of glucose, a direct precursor in cellulose biosynthesis. Glucose, dextrose, and fructose, as simple sugars, are metabolized more efficiently than disaccharides like sucrose, accelerating the formation of UDP-glucose [29]. Although glucose and dextrose are chemically identical, both were used in this study to reflect their different commercial uses and to explore any practical variation in BC production. In RTC-SD and RTC-SGlu, sucrose was likely hydrolyzed by invertase into glucose and fructose, with glucose preferentially utilized [31]. As shown in **Table 2**, higher carbon consumption in these treatments likely contributed to increased BC production.

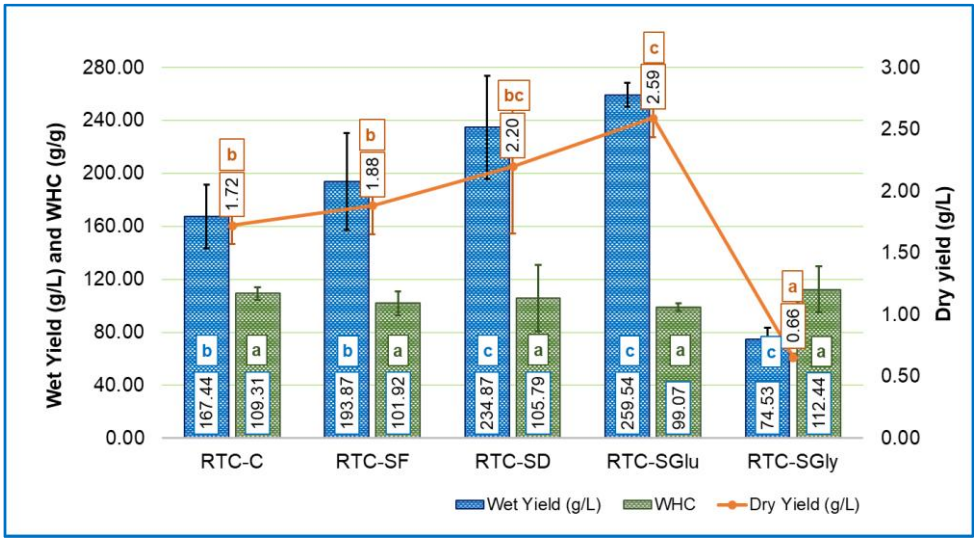


**Figure 2** Wet yield (g/L), dry yield (g/L), and water holding capacity (WHC) (g water/g cellulose) of BC produced from RTC kombucha using different combinations of carbon sources. Different lowercase letters indicate significant differences among treatments ($p < 0.05$, LSD test).

RTC-SF showed a moderate but non-significant yield increase compared to the control. While fructose supports BC formation, its efficiency is generally lower than glucose [29]. The control (RTC-C) produced lower yields, suggesting that monosaccharide addition improves sugar utilization and BC synthesis. RTC-SGly had the lowest yields, indicating glycerol was least effective under the tested conditions, possibly due to slower conversion into cellulose precursors or inhibitory effects. Although previous studies reported high yields with glycerol [37-42], variations in strains, pH, or media likely account for the difference. These findings align with [8], who reported the highest BC yields with glucose and dextrose (301.81 g/L and 11.19 g/L; 300.74 g/L and 12.12 g/L, respectively), followed by fructose and sucrose. Similarly, [13] reported that glucose resulted in higher BC yields compared to other carbon sources such as raffinose and glycerol. *K. rhaeticus* produced a maximum BC yield (~8.7 g/L) at 3% glycerol, but the yield declined at concentrations above 4% [40]. Likewise, Adnan *et al.* [43] observed that BC production peaked at 2% glycerol, with a subsequent decrease at concentrations of 3% and higher [43].

WHC showed no significant differences among treatments, indicating the carbon source primarily affects yield, not water-holding ability. WHC depends more on nanofiber structure, porosity, and surface area, which remained consistent across conditions. Values (99.07 - 112.44 g/g) were consistent with literature: 98.5 g/g from distillery wastewater [44], ~114 g/g from black tea kombucha [45], and 90 - 200 g/g ranges reported elsewhere [8,46-48]. In summary, while the carbon source influenced BC yield, it did not affect WHC, which remained a stable property across conditions.

***Morphology analysis***

**Figure 3** shows SEM images of BC produced with different carbon sources. All samples were captured at 10,000× and 30,000× magnification, while RTC-C and RTC-SGlu were also imaged at 50,000× for a closer look at their fiber structures. The BC samples display a consistent fiber pattern, aligning with previous studies [49-51].

The SEM images reveal how different carbon sources affect BC structure. Overall, glucose (RTC-SGlu) and dextrose (RTC-SD) produce denser, more organized networks, while glycerol (RTC-SGly) results in a looser structure. The thicker BC layers in RTC-SD and RTC-SGlu before drying likely contribute to their denser fibrils, aligning with their higher wet yields. In contrast, RTC-SGly's thinner network reflects its lower wet yield. Some impurities, especially in RTC-C, are visible in the SEM images, likely residues from alkali purification.

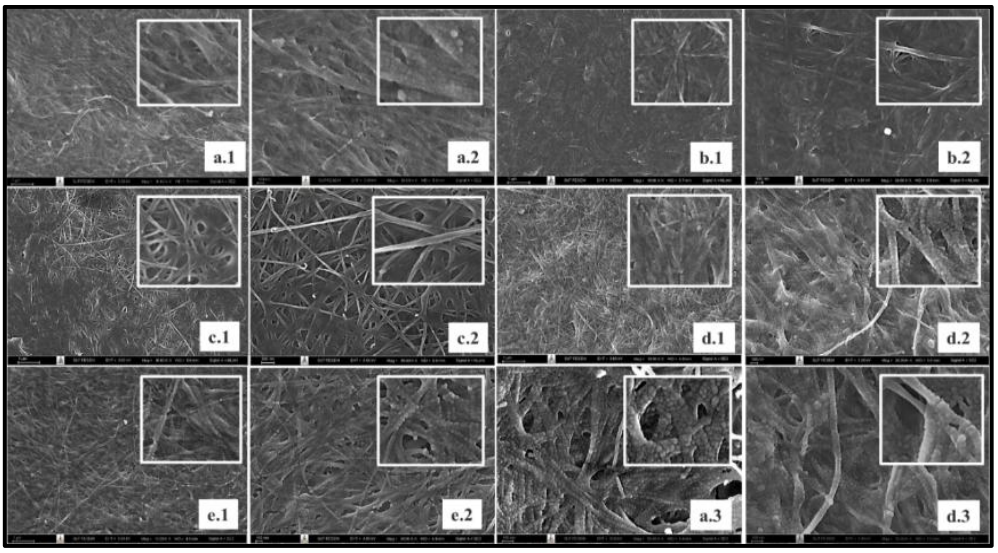


**Figure 3** SEM image of BC (a) RTC-control; (b) RTC-SF; (c) RTC-SD; (d) RTC-SG; and (e) RTC-SGly; (1) magnification of 10,000×; (2) magnification of 30,000×; (3) magnification 50,000×.

The SEM analysis focused on the polydispersity of BC fiber diameters, as illustrated in **Figure 4**. The control sample (RTC-C) exhibited the smallest average fiber diameter (29.70 nm), whereas the RTC-SD sample (sucrose and dextrose) showed the largest (40.39 nm). The RTC-SF sample (sucrose and fructose) also significantly increased the fiber diameter to 38.56 nm. Intermediate values were observed for RTC-Gly (35.86 nm) and RTC-Glu (34.34 nm). Based on LSD analysis ($p < 0.05$), RTC-Gly and RTC-Glu did not differ significantly from each other, but both exhibited significantly larger fiber diameters than the control. These results suggest that the type of sugar used as a carbon source can influence the nanofibrillar structure of BC. The broader polydispersity observed in **Figure 4** for sugar-treated samples further supports the impact of the carbon source on BC fiber morphology.

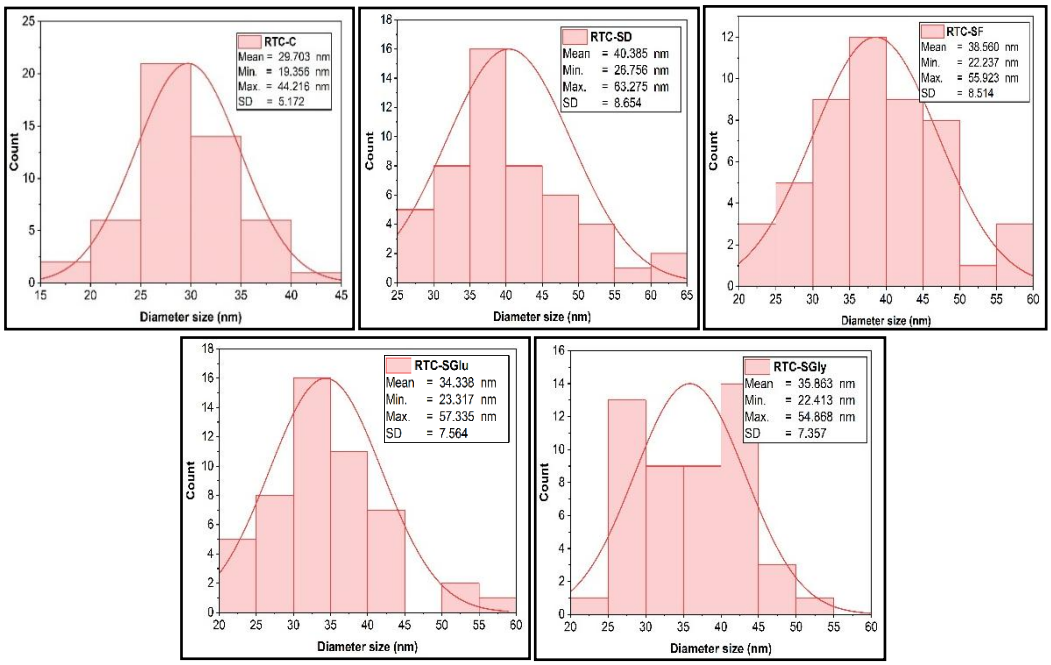


**Figure 4** Graph of poly distribution size of BC samples diameter from RTC kombucha fermentation with various types of carbon source combinations.

These findings align with previous studies. BC fibers produced by *K. hansenii* and a strain from grape juice ranged from 10 to 60 nm [49], while *K. saccharivorans* in HS medium with palm date supplementation had diameters between 10 and 90 nm [52]. Similarly, BC nanofibers from HS medium ranged from 18 to 69 nm (avg. 36 nm), and those from waste fig medium ranged from 23 to 90 nm (avg. 44 nm) [53]. Low-cost media, such as date syrup and cheese whey, synthesized BC with an average diameter of 45 - 55 nm [54]. Overall, the BC fiber diameters from Thai red tea kombucha align with those from various strains and media, indicating similar morphological characteristics.

***Fourier transform infrared spectroscopy***

**Figure 5** presents the FTIR spectra of BC samples derived from RTC kombucha fermentation using various carbon sources. All samples display similar absorption bands, although their intensities differ. The spectra confirm characteristic cellulose absorption bands, with variations in band intensity consistent with previous studies [55-57].

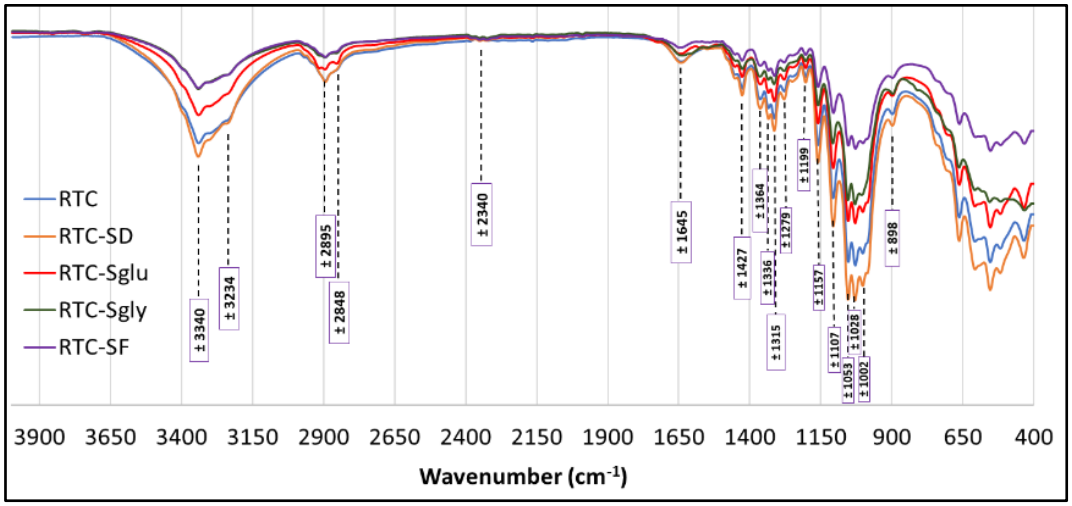


**Figure 5** FTIR spectra of BCs from RTC kombucha fermentation with various of carbon sources combinations.

The spectra are divided into the feature region (4,000 - 1,330 $cm^{-1}$) and the fingerprint region (1,330 - 500 $cm^{-1}$) [58]. In the feature region, absorption bands at ~3,340 $cm^{-1}$ and 3,234 $cm^{-1}$ correspond to O–H stretching vibrations, with intensity differences indicating variations in hydrogen bonding. The band at 2,895 $cm^{-1}$, attributed to C–H stretching, shows slightly reduced absorption in RTC-SD, suggesting altered C–H interactions. A faint band at ~2,340 $cm^{-1}$ may indicate the presence of C≡C or C≡N functional groups, potentially originating from polyphenols, fermentation byproducts, or microbial activity in kombucha [59].

In the 1,350 - 2,000 $cm^{-1}$ range, bands at 1,645 $cm^{-1}$ (C=O stretching), 1,427 $cm^{-1}$ ($CH_2$ symmetric bending), and 1,364 $cm^{-1}$ (C–H symmetric bending) further characterize the BC structure [60,61]. The fingerprint region features bands at 1,315 $cm^{-1}$ ($CH_2$ wagging or C–OH deformation), 1,247 $cm^{-1}$ (unidentified, but similar to BC produced from glucose and other sugars), 1,159 $cm^{-1}$ (C–O–C antisymmetric bridge stretching), 1,106 $cm^{-1}$ (ring asymmetric stretching), 1,053 and 1,028 $cm^{-1}$ (C–O–C and C–O–H stretching), and 898 - 894 $cm^{-1}$ (C–O–C stretching in β-1,4-glycosidic linkages), indicating an amorphous cellulose structure [58,62].

***X-Ray diffraction analysis***

The XRD patterns of BC samples from Thai red tea fermentation with different carbon sources are shown in **Figure 6**, with crystallinity index (CI) and crystallite size detailed in **Table 3**. All samples exhibit three distinct peaks at $2\theta \approx 14.74°$, 17.03° and 22.90°, corresponding to the 100, 110, and 200 planes of

cellulose type I [63,64]. The strongest peak near 23° confirms the crystalline structure of cellulose type I [64,65], confirming its crystalline nature [66]. While band positions are consistent, variations in relative intensities and crystallinity indicate differences in cellulose chain orientation and structural properties [64].

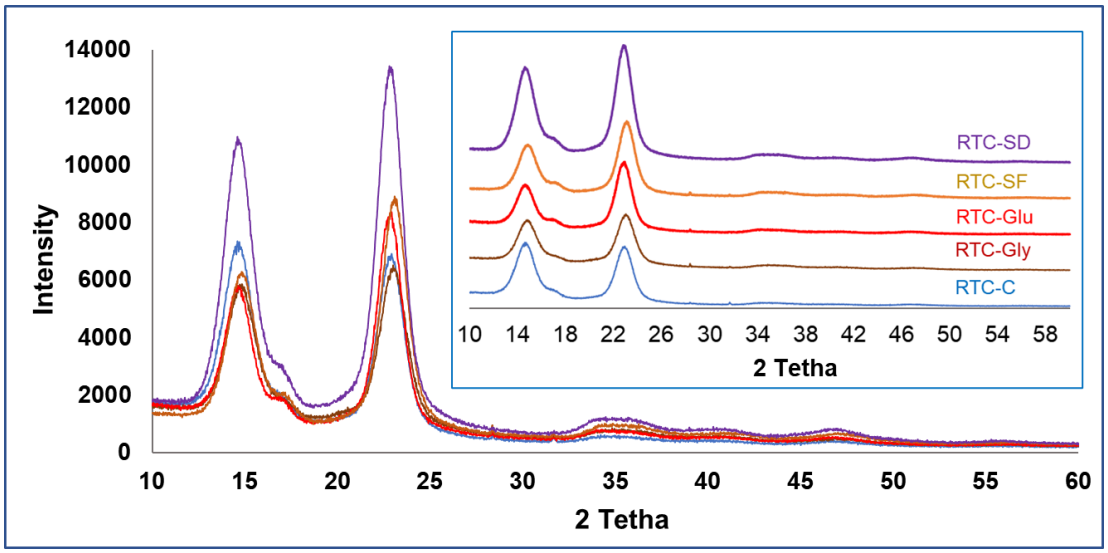


**Figure 6** XRD spectra of BC from Thai red tea kombucha with different carbon source combinations.

The crystallinity index (CI) and crystallite size of BC samples were determined from XRD data using the Segal method (**Table 3**). CI values ranged from 84.74% (RTC-SGly) to 89.54% (RTC-C), with RTC-SD and RTC-SF showing relatively similar values. All mixed carbon source samples had lower CI than sucrose-only RTC-C. BC crystallinity depends on multiple factors, including carbon/nitrogen sources, additives, bacterial strain, fermentation conditions, and post-processing [67,68]. These results agree with previous studies: *K. medellinensis* produced BC with 83% - 90% CI using different sugars [69], *K. hansenii* achieved >80% CI with glucose/glycerol [13], and *Komagataeibacter* sp. W1 showed 74% - 89% CI across various carbon sources [55]. These findings confirm that carbon source selection significantly impacts BC's crystallinity and structural properties.

**Table 3** Crystallinity index and average crystallite size of dried BC from Thai red tea kombucha fermentation with different additives.

| Samples | Crystallinity Index (%) | Average Crystallite Size (nm) |
|---|---|---|
| RTC-C | 89.54 | 3.194 |
| RTC-SF | 88.35 | 3.112 |
| RTC-SD | 88.17 | 3.181 |
| RTC-SGlu | 86.00 | 3.327 |
| RTC-SGly | 84.74 | 3.069 |

Analysis was performed once; no replication was conducted for this measurement.

Building on the crystallinity findings, the crystallite size analysis revealed similar dependencies on carbon sources and fermentation conditions. Our BC samples showed crystallite sizes ranging from 3.07 to 3.33 nm (**Table 3**), consistent with the 3.06 nm crystals reported for *G. xylinus* [70]. The observed variations

align well with literature values: *K. xylinus* produced larger crystallites (4.7 - 6.8 nm) using simple sugars [71], while *Lactobacillus plantarum* in green tea medium formed 5.36 - 5.98 nm crystallites over extended fermentation [72]. Other studies report comparable ranges, from black tea kombucha BC (3.29 - 4.80 nm) [73] to larger crystallites (4.76 - 8.36 nm) under different conditions [17,74,75]. Overall, these findings suggest that while crystallite size remains within a narrow range, it is subtly influenced by the type of carbon source and the resulting microbial activity during fermentation.

***Thermogravimetric analysis (TGA/DTG)***

**Figure 7** shows the thermogravimetric (TG) (**Figure 7(a)**) and derivative thermogravimetric (DTG) (**Figure 7(b)**) curves of BC samples (RTC-C, RTC-SF, RTC-SD, RTC-Glu, RTC-Gly), with decomposition data summarized in **Table 4**. These results illustrate the thermal stability and degradation behavior of BC, which are essential for applications requiring chemical resistance and strong fiber–matrix interactions [76]

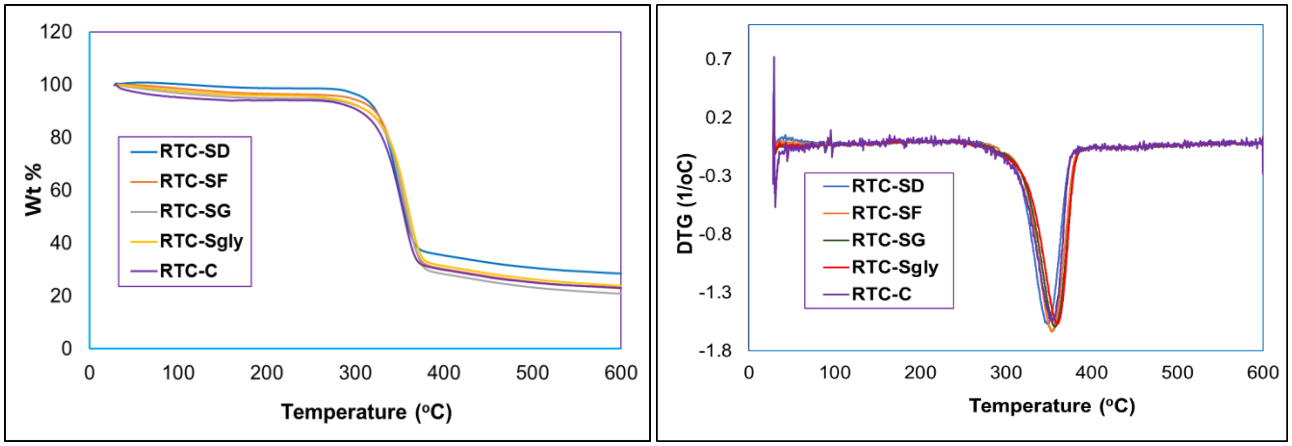


**Figure 7** TGA (a) and DTG (b) thermographs of BC samples from Thai red tea fermentation with different combinations of carbon sources.

**Table 4** The details of data decomposition during the TGA process of BC samples from kombucha fermentation with different types of tea.

| Samples | First stage weight loss (%) | Second stage weight loss (%) | Residue (%) | DTG peak range (°C) | DTG $T_{Max}$ (°C) |
|---|---|---|---|---|---|
| RTC-C | 6.03 | 71.01 | 23.01 | 256 - 384 | 353.67 |
| RTC-SD | 1.34 | 70.10 | 28.52 | 260 - 391 | 349.50 |
| RTC-SF | 3.60 | 73.43 | 22.94 | 267 - 390 | 353.33 |
| RTC-SGlu | 5.14 | 73.90 | 20.92 | 268 - 389 | 356.83 |
| RTC-SGly | 4.15 | 71.92 | 23.90 | 258 - 388 | 359.50 |

Analysis was performed once; no replication was conducted for this measurement.

The first-stage weight loss, ranging from 1.34% to 6.03%, corresponds to moisture loss and the volatilization of low-molecular-weight components [77,78]. RTC-SD exhibited the lowest weight loss (1.42%), suggesting reduced moisture retention, a result consistent with previous studies reporting first-stage losses of 1% - 2% [1] and 5% - 9% [77]. The second-stage weight loss, associated with cellulose decomposition, ranged from 70.10% in RTC-SD to 73.90% in RTC-SGlu. Residual weights at 600 °C

varied from 20.92% (RTC-SGlu) to 28.52% (RTC-SD), indicating differences in the formation of thermally stable by-products. This stage causes the biggest weight loss, mainly due to the breakdown of β-glucan chains and the oxidation of cellulose into carbon residues [77,80].

These findings are consistent with previous studies. For example, BC from *Acetobacter xylinum* AGR 60 exhibited a two-stage thermal decomposition: An initial weight loss of 6%, followed by a second-stage loss of 74%, leaving 20% residue at 700 °C. The main decomposition occurred between 300 °C and 360 °C [81]. Similarly, BC from *Gluconacetobacter xylinus* AGR 60 showed a 6.2% first-stage loss, a 64% second-stage loss, and 22.8% residue at 600 °C, with a DTG_max of 339.6 °C [82]. BC synthesized from different carbon sources—glucose, fructose, sucrose, and glycerol—also displayed a comparable decomposition pattern, with residual mass ranging from 15.2% to 23.1% at 600 °C [83]. In contrast, BC produced from green tea kombucha undergoes three decomposition stages at 152, 267 and 359 °C, resulting in a total weight loss of 74.42% and a residue of 25.58%, which differs from the two-stage decomposition observed in the present study [84].

DTG analysis showed a peak temperature range of 256 - 391 °C, with maximum degradation temperatures (DTG Max) between 349.50 °C and 359.50 °C. RTC-SGly exhibited the highest DTG Max (359.50 °C), suggesting slightly enhanced thermal stability. Comparisons with previous studies indicate some variation in DTG Max values, such as 328.36 °C for *G. xylinus* BC [74], 354.5 - 355.4 °C for *G. hansenii* BC in HS medium [85], and 327 - 368 °C for *K. medellinensis* BC from various waste sources [86]. Additionally, BC treated with freeze-drying and hot-press drying methods yielded DTG Max values of 343.6 °C and 313.4 °C, respectively, with DTG peak ranges of 186 - 363 °C and 199 - 347 °C [77]. BC produced through kombucha fermentation of green tea showed a DTG Max of 366 °C [84]. Overall, while RTC-SGly demonstrated the highest DTG Max in this study, the narrow range of differences suggests that carbon source selection has a relatively minor impact on the thermal properties of BC.

***Nano-indentation analysis***

Nano-indentation was used to evaluate the mechanical properties of BC samples at the nanoscale. Samples RTC-SD and RTC-SGlu, selected for their high yields, were compared with the control (RTC-C) (**Table 5**). No significant differences were found in maximum depth, plastic indentation depth, hardness, reduced modulus, or Young's modulus ($p > 0.05$), indicating that the carbon source—sucrose alone or combined with dextrose or glucose—had minimal impact. While carbon sources can influence BC properties [87,88], this effect was not statistically significant here.

**Table 5** Mechanical properties of BC from kombucha fermentation of RTC-SD, RTC-SGlu, and RTC-C analyzed using a nano-indenter.

| Sample | MD (nm) | Pl (nm) | ML (mN) | H (GPa) | RM (GPa) | ERP | CC (nm/mN) | PW (nJ) | EW (nJ) | YM (GPa) |
|---|---|---|---|---|---|---|---|---|---|---|
| RTC-SD | 3402.68 ± 388.52 | 2950.54 ± 366.31 | 50.10 ± 0.00 | 0.23 ± 0.07 | 4.844 ± 1.02 | 0.16 ± 0.02 | 12.03 ± 0.82 | 49.29 ± 5.30 | 21.67 ± 1.40 | 4.43 ± 0.94 |
| RTC-SGlu | 3206.75 ± 250.54 | 2754.19 ± 240.80 | 50.10 ± 0.00 | 0.26 ± 0.05 | 5.106 ± 0.64 | 0.17 ± 0.01 | 12.04 ± 0.65 | 51.22 ± 4.42 | 21.08 ± 1.08 | 4.67 ± 0.59 |
| RTC-C | 3412.25 ± 259.56 | 2980.18 ± 253.91 | 50.10 ± 0.00 | 0.22 ± 0.05 | 4.94 ± 0.56 | 0.15 ± 0.01 | 11.50 ± 0.22 | 54.41 ± 4.64 | 20.80 ± 0.47 | 4.51 ± 0.51 |

MD: maximum depth, Pl: plastic, ML: maximum load, H: hardness, RM: reduced modulus, ERP: elastic recovery parameters, CC: contact compliance, PW: plastic work, EW: elastic work, and YM: Young's Modulus. Based on the statistical analysis, there were no significant differences among the samples across all parameters ($p > 0.05$).

The mechanical properties of bacterial cellulose (BC) are affected by various factors, including the type of microorganism, how the BC is grown, how it is purified, and how it is dried [87-91]. Using different concentrations of NaOH during purification can damage or preserve the fiber structure [92,93]. The drying method also changes the porosity, density, and fiber arrangement of the final product [90,94]. Crystallinity is another important factor. A higher CI usually leads to greater stiffness and Young's modulus but lower flexibility [57,95]. In this study, all treatments had similar CI values, which match their similar Young's modulus values.

The measured Young's modulus values fall within ranges reported in the literature: 1.10 - 5.56 GPa for *Komagataeibacter* strains [91], up to 9.14 GPa for *A. xylinum* AGR60 in coconut water [81], and $8.0 \pm 1.9$ GPa in kombucha-derived BC [96]. In conclusion, while carbon sources can affect mechanical behavior, crystallinity and other processing factors appeared to play a more dominant role in this study.

This study reveals that substituting part of the sucrose with either glucose or dextrose significantly improves BC production in terms of both wet and dry yield. The sucrose-only control (RTC-C) produced a lower yield compared to the RTC-SGlu and RTC-SD combinations, indicating enhanced fermentation efficiency with the addition of these monosaccharides. Although glucose and dextrose yielded similar results, the lower cost of dextrose makes it a more practical and economical option for large-scale production. In contrast, sucrose alone was less effective, suggesting limited suitability as a sole carbon source under these conditions.

From a value perspective, the increase in BC yield translates to more efficient fiber production, which is critical for applications requiring high quantities of cellulose material. While the addition of glucose or dextrose increases the raw material cost compared to using sucrose alone, the improvement in yield—particularly when using the more affordable dextrose—can offset this cost in industrial settings. Glucose, though slightly more expensive, remains valuable for controlled research environments due to its predictable behavior during fermentation. Overall, these findings support the use of sucrose–dextrose or glucose combinations as the cost-effective and high-performing formulation for optimizing BC yield and scalability. Future optimization and cost-benefit analysis will further clarify the best carbon source strategies for commercial BC production.

## Conclusions

This study demonstrated that carbon source combinations significantly influenced BC production from Thai red tea kombucha, with wet yields ranging from 74.53 g/L (RTC-SGly) to 259.54 g/L (RTC-SGlu) and dry yields from 0.66 g/L to 2.59 g/L. Water-holding capacity ranged from 99.07 to 112.44 g/g, and fiber diameters from $29.70 \pm 5.17$ nm (control) to $40.39 \pm 8.65$ nm (RTC-SD), while all samples exhibited comparable functional groups and crystallinity (84.74% - 89.54%). Thermal and mechanical properties showed no significant differences among treatments. These findings highlight that combining sucrose with glucose or dextrose can substantially boost BC yield without compromising its structural and functional integrity.

## Acknowledgements

We gratefully acknowledge the financial support for this research provided by Suranaree University of Technology (SUT), Thailand Science Research and Innovation (TSRI), the National Science, Research and Innovation Fund (NSRF) under contract no. 195650, and the National Research and Innovation Agency, Indonesia (BRIN).

## Declaration of generative AI in scientific writing

This manuscript was edited for language and readability using generative AI tools under human supervision. The authors take full responsibility for its content.

## CRediT author statement

**Wawan Agustina**: conceptualization, methodology, writing—original draft, and visualization. **Apichat Boontawan**: writing - review & editing, supervision, and funding acquisition.

**References**


[1] D Lin, Z Liu, R. Shen, S Chen and X Yang. Bacterial cellulose in food industry: Current research and future prospects. *International Journal of Bioliogical Macromolecules* 2020; **158**, 10007-1019.

[2] C Zhong. Industrial-Scale Production and Applications of Bacterial Cellulose. *Frontiers in Bioengineering and Biotechnology* 2020; **8**, 605374.

[3] L Rosson, B Tan, W Best and N Byrne. Applications of regenerated bacterial cellulose: A review. *Cellulose* 2024; **31**, 10165-10190.

[4] D Absharina, M Padri, C Veres and C Vagvolgyi. Bacterial Cellulose: From biofabrication to applications in sustainable fashion and vegan leather. *Fermentation* 2025; **11(1)**, 23.

[5] R Mehrotra, S Sharma, N Shree and K Kaur. Bacterial cellulose: An ecological alternative as a biotextile. *Biosciences Biotechnology Research Asia* 2023; **20(2)**, 449-463.

[6] X Feng, Z Ge, Y Wang, X Xia, B Zhao and M Dong. Production and characterization of bacterial cellulose from kombucha-fermented soy whey. *Food Production, Processing and Nutrition* 2024; **6**, 20.

[7] LFA Amorim, L Li, AP Gomes, R Fangueiro and IC Gouveia. Sustainable bacterial cellulose production by low-cost feedstock: Evaluation of apple and tea by-products as alternative sources of nutrients. *Cellulose* 2023; **30**, 5589-5606.

[8] MZ Treviño-Garza, AS Guerrero-Medina, RA Gonzalez-Sanchez, C Garcia-Gomez, A Guzman-Velasco, JG Baez-Gonzalez and JM Marquez-Reyes. Production of microbial cellulose films from green tea (*Camellia Sinensis*) kombucha with various carbon sources. *Coating* 2020; **10(11)**, 1132.

[9] G Buldum and A Mantalaris. Systematic understanding of recent developments in bacterial cellulose biosynthesis at genetic bioprocess and product levels. *International Journal of Molecular Sciences* 2021; **22(13)**, 7192.

[10] A Pandey, A Singh and MK Singh. Novel low-cost green method for production bacterial cellulose. *Polymer Bulletin* 2024; **81**, 6721-6741.

[11] B Hungund, S Prabhu, C Shetty, S Acharya, V Prabhu, and SG Gupta. Production of bacterial cellulose from *Gluconacetobacter persimmonis* GH-2 using dual and cheaper carbon sources. *Journal of Microbial & Biochemical Technology* 2013; **5(2)**, 31-33.

[12] G Singh, P Gauba and G Mathur. Bacterial Cellulose Production by *Acetobacter aceti* MTCC 2623 Using Different Carbon Sources. *Current Applied Science and Technology* 2024; **24(6)**, 0260805.

[13] J Amorim, K Liao, A Mandal, AF de S Costa, E Roumeli and LA Sarubbo. Impact of carbon source on bacterial cellulose network architecture and prolonged lidocaine release. *Polymers* 2024; **16(21)**, 3021.

[14] K Aswini, NO Gopal and S Uthandi. Optimized culture conditions for bacterial cellulose production by *Acetobacter senegalensis* MA1. *BMC Biotechnology* 2020; **20(1)**, 46.

[15] ST Schrecker and PA Gostomski. Determining the water holding capacity of microbial cellulose. *Biotechnology letters* 2005; **27**, 1435-1438.

[16] TG Volova, SV Prudnikova, EG Kiselev, IV Nemtsev, AD Vasiliev, AP Kuzmin and EI Shishatskaya. Bacterial Cellulose (BC) and BC Composites: Production and Properties. *Nanomaterials* 2022; **12(2)**, 192.

[17] SA Sardjono, H Suryanto, Aminnudin and M Muhajir. Crystallinity and morphology of the bacterial nanocellulose membrane extracted from pineapple peel waste using high-pressure homogenizer. *AIP Conference Proceedings* 2019; **2120(1)**, 080015.

[18] RJ Roberts, RC Rowe and P York. The Poisson's ratio of microcrystalline cellulose. *International Journal of Pharmaceutics* 1994; **105(2)**, 177-180.

[19] FA Rabbani, S Yasin, T Iqbal and U Farooq. Experimental Study of mechanical properties of polypropylene random copolymer and Rice-Husk-Based biocomposite by using nanoindentation. *Materials (Basel)* 2022; **15(5)**, 1956.

[20] KR Lee, K Jo, KS Ra, HJ Suh and K Hong. Kombucha fermentation using commercial kombucha pellicle and culture broth as starter. *Food Science and Technology* 2022; **42**, 70020.

[21] K Neffe-Skocińska, B Sionek, I Ścibisz and D Kołożyn-Krajewska. Acid contents and the effect

of fermentation condition of Kombucha tea beverages on physicochemical, microbiological and sensory properties. *CyTA - Journal of Food* 2017; **15(4)**, 1321588.

[22] B Vohra, S Fazry, F Sairi and BA Othman. Effects of medium variation and fermentation time towards the pH level and ethanol content of Kombucha. *AIP Conference Proceedings* 2019; **2111**, 040008.

[23] AQ Chong, NL Chin, RA Talib and RK Basha. Modelling pH dynamics, SCOBY biomass formation, and acetic acid production of kombucha fermentation using black, green, and oolong teas. *Processes* 2024; **12(7)**, 1301.

[24] M Muzaifa, S Rohaya, C Nilda and KR Harahap. Kombucha fermentation from cascara with addition of red dragon fruit (*Hylocereus polyrhizus*): Analysis of alcohol content and total soluble solid. *In*: Proceedings of the International Conference on Tropical Agrifood, Feed and Fuel, Samarinda East Kalimantan, Indonesia.

[25] E Zubaidah, RA Ifadah and CA Afgani. Changes in chemichal characteristics of kombucha from various cultivars of snake fruit during fermentation. *International Conference on Green Agro-industry and Bioeconomy* 2019; **230**, 012098.

[26] KN Sinamo, S Ginting and S Pratama. Effect of sugar concentration and fermentation time on secang kombucha drink. *IOP Conference Series: Earth and Environmental Science* 2022; **977**, 012080.

[27] E Ball. Hydrolysis of sucrose by autoclaving media, a neglected aspect in the technique of culture of plant tissues. *Bulletin of the Torrey Botanical Club* 1953; **80(5)**, 409-411.

[28] JH de Lange. Significance of autoclaving-induced toxicity from and hydrolysis of carbohydrates in *in vitro* studies of pollen germination and tube growth. *South African Journal of Botany* 1989; **55(1)**, 1-5.

[29] M Gao, D Ploessl and Z Shao. Enhancing the co-utilization of biomass-derived mixed sugars by yeasts. *Frontiers in Microbiology* 2018; **9**, 03264.

[30] J Lee. Exploring sucrose fermentation: Microorganisms, Biochemical Pathways, and Applications. *Fermentation Technology* 2023; **12(1)**, 1000166.

[31] B Wang, K Rutherfurd-Markwick, XX Zhang and AN Mutukumira. Kombucha: Production and microbiological research. *Foods* 2022; **11(21)**, 3456.

[32] H Deka, PP Sarmah, A Devi, P Tamuly and T Karak. Changes in major catechins, caffeine, and antioxidant activity during CTC processing of black tea from North East India. *RSC Advances* 2021; **11(19)**, 11457-11467.

[33] A Ito and E Yanase. Study into the chemical changes of tea leaf polyphenols during japanese black tea processing. *Food Research International* 2022; **160**, 111731.

[34] K Izawa, Y Amino, M Kohmura, Y Ueda and M Kuroda. Human-environment interactions – taste. *Comprehensive Natural Products II: Chemistry and Biology* 2010; **4**, 631-671.

[35] AS Amarasekara, D Wang, and TL Grady. A comparison of kombucha SCOBY bacterial cellulose purification methods. *SN Applied Sciences* 2020; **2**, 240.

[36] ASM Kamal, MI Misnon and F Fadil. The effect of sodium hydroxide concentration on yield and properties of Bacterial Cellulose membranes. *IOP Conference Series: Materials Science and Engineering* 2020; **732**, 012064.

[37] SMAS Keshk and K Sameshima. Evaluation of different carbon sources for bacterial cellulose production. *African Journal of Biotechnology* 2005; **6(4)**, 478-482.

[38] JDP Amorim, AFS Costa, CJS Galdino, GM Vinhas, EMS Santos and LA Sarubbo. Bacterial cellulose production using fruit residues as substract to industrial application. *Chemical Engineering Transactions* 2019; **74**, 1165-1170.

[39] YH Jin, T Lee, JR Kim, YE Choi and C Park. Improved production of bacterial cellulose from waste glycerol through investigation of inhibitory effects of crude glycerol-derived compounds by *Gluconacetobacter xylinus*. *Journal of Industrial and Engineering Chemistry* 2019; **75**, 158-163.

[40] MN Thorat and SG Dastager. High yield production of cellulose by a: *Komagataeibacter rhaeticus* PG2 strain isolated from pomegranate as a new host. *RSC Advances* 2018; **52**, 29797-29805.

[41] MJ Tabaii and G Emtiazi. Comparison of bacterial cellulose production among different strains and fermented media. *Applied Food Biotechnology* 2016; **3(1)**, 35-41.

[42] YE Agustin, KS Padmawijaya, HF Rixwari and VAS Yuniharto. Glycerol as an additional carbon source for bacterial cellulose synthesis. *IOP Conference Series: Earth and Environmental Science* 2018; **141**, 012001.

[43] A Adnan, GR Nair, MC Lay, JE Swan, and R Umar. Glycerol as a cheaper carbon source in Bacterial Cellulose (BC) production by *Gluconacetobacter xylinus* Dsm46604 in Batch Fermentation System. *Malaysian Journal of Analytical Sciences* 2015; **19(5)**, 1131-1136.

[44] JM Wu and RH Liu. Cost-effective production of bacterial cellulose in static cultures using distillery wastewater. *Journal of Bioscience and Bioengineering* 2013; **115(3)**, 284-290.

[45] NH Avcioglu, M Birben and IS Bilkay. Optimization and physicochemical characterization of enhanced microbial cellulose production with a new Kombucha consortium. *Process Biochemistry* 2021; **108**, 60-68.

[46] E Tsouko, C Kourmentza, D Ladakis, N Kopsahelis, I Mandala, S Papanikolaou, F Paloukis, V Alves and A Koutinas. Bacterial cellulose production from industrial waste and by-product streams. *International Journal of Molecular Sciences* 2015; **16(7)**, 14832-14849.

[47] RAH Almihyawi, E Musazade, N Alhussany, S Zhang and H Chen. Production and characterization of bacterial cellulose by Rhizobium sp. isolated from bean root. *Scientific Reports* 2024; **14**, 10848.

[48] C Ugurel and H Ogut. Optimization of bacterial cellulose production by *Komagataeibacter rhaeticus* K23. *Fibers* 2024; **12(3)**, 29.

[49] MP Illa, M Khandelwal and CS Sharma. Modulated dehydration for enhanced anodic performance of bacterial cellulose derived carbon nanofibers. *ChemistrySelect* 2019; **21(4)**, 6642-6650.

[50] TA Nguyen and XC Nguyen. Bacterial Cellulose-Based biofilm forming agent extracted from vietnamese nata-de-coco tree by ultrasonic vibration method: Structure and properties. *Journal of Chemistry* 2022; **2022(1)**, 7502796.

[51] R Brandes, L De Souza, C Carminatti and D Recouvreux. Production with a high yield of bacterial cellulose nanocrystals by enzymatic hydrolysis. *International Journal of Nanoscience* 2020; **19(3)**, 1950015.

[52] D Abol-Fotouh, MA Hassan, H Shokry, A Roig, MS Azab and AEHB Kashyout. Bacterial nanocellulose from agro-industrial wastes: Low-cost and enhanced production by *Komagataeibacter saccharivorans* MD1. *Scientific Reports* 2020; **10**, 3491.

[53] M Yilmaz and Y Goksungur. Optimization of bacterial cellulose production from waste figs by *Komagataeibacter xylinus*. *Fermentation* 2024; **10(9)**, 466.

[54] Y Raiszadeh-Jahromi, M Rezazadeh-Bari, H Almasi and S Amiri. Optimization of bacterial cellulose production by *Komagataeibacter xylinus* PTCC 1734 in a low-cost medium using optimal combined design. *Journal of Food Science and Technology* 2020; **57(7)**, 2524-2533.

[55] SS Wang, YH Han, JL Chen, DC Zhang, XX Shi, YX Ye, DL Chen and M Li. Insights into bacterial cellulose biosynthesis from different carbon sources and the associated biochemical transformation pathways in *Komagataeibacter* sp. W1. *Polymers (Basel)* 2018; **10(9)**, 963.

[56] NAM Razali, RM Sohaimi, RNIR Othman, N Abdullah, SZN Demon, L Jasmani, WMZW Yunus, WMHW Ya'acob, EM Salleh, MN Norizan and NA Halim. Comparative study on extraction of cellulose fiber from rice straw waste from chemo-mechanical and pulping method. *Polymers (Basel)* 2022; **14(3)**, 387.

[57] MA Adekoya, S Liu, SS Oluyamo, OT Oyeleye and RT Ogundare. Influence of size classifications on the crystallinity index of *Albizia gummifera* cellulose. *Heliyon* 2022; **8(12)**, 12019.

[58] X Liu, L Cao, S Wang, L Huang, Y Zhang, M Tian, X Li and J Zhang. Isolation and characterization of bacterial cellulose produced from soybean whey and soybean hydrolyzate. *Scientific Reports* 2023; **13**, 16024.

[59] S Srivastava and G Mathur. *Komagataeibacter saccharivorans* strain BC-G1: An alternative strain for production of bacterial cellulose.

*Biologia (Bratisl)* 2022; **77**, 3657-3668.

[60] E Leonarski, K Cesca, E Zanella, BU Stambuk, D de Oliveira and P Poletto. Production of kombucha-like beverage and bacterial cellulose by acerola byproduct as raw material. *LWT* 2021; **135**, 110075.

[61] A Fatima, P Ortiz-Albo, LA Neves, FX Nascimento and JG Crespo. Biosynthesis and characterization of bacterial cellulose membranes presenting relevant characteristics for air/gas filtration. *Journal of Membrane Science* 2023; **674**, 121509.

[62] D Ciolacu, F Ciolacu and VI Popa. Amorphous cellulose - structure and characterization. *Cellulose Chemistry and Technology* 2011; **45(1-2)**, 13-21.

[63] D Gaspar, SN Fernandes, AG De Oliveira, JG Fernandes, P Grey, RV Pontes, L Pereira, R Martins, MH Godinho and E Fortunato. Nanocrystalline cellulose applied simultaneously as the gate dielectric and the substrate in flexible field effect transistors. *Nanotechnology* 2014; **25(9)**, 094008.

[64] SNNS Azmi, Z'Asyiqin Samsu, ASFM Asnawi, H Ariffin and SS Syed Abdullah. The production and characterization of bacterial cellulose pellicles obtained from oil palm frond juice and their conversion to nanofibrillated cellulose. *Carbohydrate Polymer Technologies and Applications* 2023; **5**, 100327.

[65] T Hossen, CK Kundu, BRR Pranto, MS Rahi, R Chanda, S Mollick, AB Siddique and HA Begum. Synthesis, characterization, and cytotoxicity studies of nanocellulose extracted from okra (*Abelmoschus esculentus*) fiber. *Heliyon* 2024; **10(3)**, 25270.

[66] OS Samuel and AM Adefusika. *Influence of size classifications on the structural and solid-state characterization of cellulose materials*. *In*: R Pascual and MEE Martin (Eds.). Cellulose. IntechOpen, London, 2019.

[67] X Zeng, J Liu, J Chen, Q Wang, Z Li and H Wang. Screening of the common culture conditions affecting crystallinity of bacterial cellulose. *Journal of Industrial Microbiology and Biotechnology* 2011; **38(12)**, 1993-1999.

[68] K Thielemans, YD Bondt, L Comer, J Raes, N Everaert, BF Sels and CM Courtin. Decreasing the crystallinity and degree of polymerization of cellulose increases its susceptibility to enzymatic hydrolysis and fermentation by colon microbiota. *Foods* 2023; **12(5)**, 1100.

[69] C Molina-Ramirez, C Enciso, M Torres-Taborda, R Zuluaga, P Ganan, OJ Rojas and C Castro. Effects of alternative energy sources on bacterial cellulose characteristics produced by *Komagataeibacter medellinensis*. *International Journal of Biological Macromolecules* 2018; **117**, 735-741.

[70] S Agustin, ET Wahyuni, Suparmo, Supriyadi and MN Cahyanto. Production and characterization of bacterial cellulose-alginate biocomposites as food packaging material. *Food Research* 2021; **5(6)**, 204-210.

[71] P Singhsa, R Narain and H Manuspiya. Physical structure variations of bacterial cellulose produced by different *Komagataeibacter xylinus* strains and carbon sources in static and agitated conditions. *Cellulose* 2018; **25**, 1571-1581.

[72] S Charoenrak, S Charumanee, P Sirisa-ard, S Bovonsombut, L Kumdhitiahutsawakul, S Kiatkarun, W Pathom-Aree, T Chitov and S Bovonsombut. Nanobacterial cellulose from kombucha fermentation as a potential protective carrier of *Lactobacillus plantarum* under simulated gastrointestinal tract conditions. *Polymers (Basel)* 2023; **15(6)**, 1356.

[73] GN Balistreri, IR Campbell, X Li, J Amorim, S Zhang, E Nance and E Roumeli. Bacterial cellulose nanoparticles as a sustainable drug delivery platform for protein-based therapeutics. *RSC Applied Polymers* 2024; **2**(**2**), 172-183.

[74] Y Jia, X Wang, M Huo, X Zhai, F Li and C Zhong. Preparation and characterization of a novel bacterial cellulose/chitosan bio-hydrogel. *Nanomaterials and Nanotechnology* 2017; **7(4)**, 184798041770717.

[75] G Gayathri and G Srinikethan. Bacterial cellulose production by *K. saccharivorans* BC1 strain using crude distillery effluent as cheap and cost-effective nutrient medium. *International Journal of Biological Macromolecules* 2019; **138**, 950-957.

[76] NM Nurazzi, MRM Asyraf, M Rayung, MNF

Norrrahim, SS Shazleen, MSA Rani, AR Shafi, HA Aisyah, MHM Radzi, FA Sabaruddin, RA Ilyas, ES Zainudin and K Abdan. Thermogravimetric analysis properties of cellulosic natural fiber polymer composites: A review on influence of chemical treatments. *Polymers (Basel)* 2021; **13(16)**, 2710.

[77] S Mohamad, LC Abdullah, SS Jamari, SSOA Edrus, MM Aung and SFS Mohamad. Production and characterization of bacterial cellulose nanofiber by *Acetobacter xylinum* 0416 using only oil palm frond juice as fermentation medium. *Journal of Natural Fibers* 2022; **19(17)**, 16005-16016.

[78] SRZ Teixeira, EMD Reis, GP Apati, MM Meier, AL Nogueira, MCF Garcia, ALDS Schneider, APT Pezzin and LM Porto. Biosynthesis and functionalization of bacterial cellulose membranes with cerium nitrate and silver nanoparticles. *Materials Research* 2019; **22(1)**, 0054.

[79] YA Gismatulina and VV Budaeva. Cellulose nitrates-blended composites from bacterial and plant-based celluloses. *Polymers (Basel)* 2024; **16(9)**, 1183.

[80] F Mohammadkazemi, M Azin and A Ashori. Production of bacterial cellulose using different carbon sources and culture media. *Carbohydrate Polymers* 2015; **117**, 518-523.

[81] K Potivara and M Phisalaphong. Development and characterization of bacterial cellulose reinforced with natural rubber. *Materials (Basel)* 2019; **12(14)**, 2323.

[82] R Jenkhongkarn and M Phisalaphong. Effect of reduction methods on the properties of composite films of bacterial cellulose-silver nanoparticles. *Polymers (Basel)* 2023; **15(14)**, 2996.

[83] BC Tureck, HG Hackbarth, EZ Neves, MCF Garcia, GP Apati, DDOS Recouvreux, APT Pezzin and ALDS Schneider. Obtaining and characterization of bacterial cellulose synthesized by *Komagataeibacter hansenii* from alternative sources of nitrogen and carbon. *Matéria (Rio de Janeiro)* 2021; **26(4)**, 1392.

[84] NF Lima, GM Maciel, IDAA Fernandes and CWI Haminiuk. Optimising the production process of bacterial nanocellulose: Impact on growth and bioactive compounds. *Food Technology and Biotechnology* 2023; **61(4)**, 494-504.

[85] VM Vasconcellos and CS Farinas. The effect of the drying process on the properties of bacterial cellulose films from *Gluconacetobacter hansenii*. *Chemical Engineering Transactions* 2018; **64**, 145-150

[86] C Molina-Ramirez, C Castro, R Zuluaga and P Ganan. Physical characterization of bacterial cellulose produced by *Komagataeibacter medellinensis* using food supply chain waste and agricultural by-products as alternative low-cost feedstocks. *Journal of Polymers and the Environment* 2018; **26**, 830-837.

[87] V Chibrikov, PM Pieczywek, J Cybulska and A Zdunek. Evaluation of elasto-plastic properties of bacterial cellulose-hemicellulose composite films. *Industrial Crops and Products* 2023; **205**, 117578.

[88] I Betlej, R Salerno-Kochan, KJ Krajewski, J Zawadzki and P Boruszewski. The influence of culture medium components on the physical and mechanical properties of cellulose synthesized by kombucha microorganisms. *BioResources* 2020; **15(2)**, 3125-3135.

[89] A Krystynowicz, W Czaja, A Wiktorowska-Jezierska, M Gonçalves-Miśkiewicz, M Turkiewicz and S Bielecki. Factors affecting the yield and properties of bacterial cellulose. *Journal of Industrial Microbiology and Biotechnolog* 2002; **29(4)**, 189-195.

[90] M Zeng, A Laromaine and A Roig. Bacterial cellulose films: Influence of bacterial strain and drying route on film properties. *Cellulose* 2014; **21**, 4455-4469.

[91] SQ Chen, P Lopez-Sanchez, D Wang, D Mikkelsen and MJ Gidley. Mechanical properties of bacterial cellulose synthesised by diverse strains of the genus *Komagataeibacter*. *Food Hydrocolloids* 2018; **81**, 87-95.

[92] H Suryanto, M Muhajir, TA Sutrisno, Mudjiono, N Zakia and U Yanuhar. The mechanical strength and morphology of bacterial cellulose films: The effect of NaOH concentration. *IOP Conference Series: Materials Science and Engineering* 2019; **515**, 012053.

[93] SQ Chen, OW Meldrum, Q Liao, Z Li, X Cao, L Guo, S Zhang, J Zhu and L Li. The influence of alkaline treatment on the mechanical and

structural properties of bacterial cellulose. *Carbohydrate Polymers* 2021; **271**, 118431.

[94] YY Wang, XQ Zhao, DM Li, YM Wu, F Wahid, YY Xie and C Zhong. Review on the strategies for enhancing mechanical properties of bacterial cellulose. *Journal of Materials Scienc*e 2023; **58**, 15265-15293.

[95] N Dusunceli and OU Colak. Modelling effects of degree of crystallinity on mechanical behavior of semicrystalline polymers. *International Journal of Plasticity* 2008; **24(7)**, 1224-1242.

[96] H Oliver-Ortega, S Geng, FX Espinach, K Oksman and F Vilaseca. Bacterial cellulose network from kombucha fermentation impregnated with emulsion-polymerized poly(methyl methacrylate) to form nanocomposite. *Polymers (Basel)* 2021; **13(4)**, 664.